Supporting Information

Small-sized and high-dispersed WN from $[SiO_4(W_3O_9)_4]^{4-}$ clusters loading on GO-derived graphene as highly-efficient carriers for methanol electro-oxidation

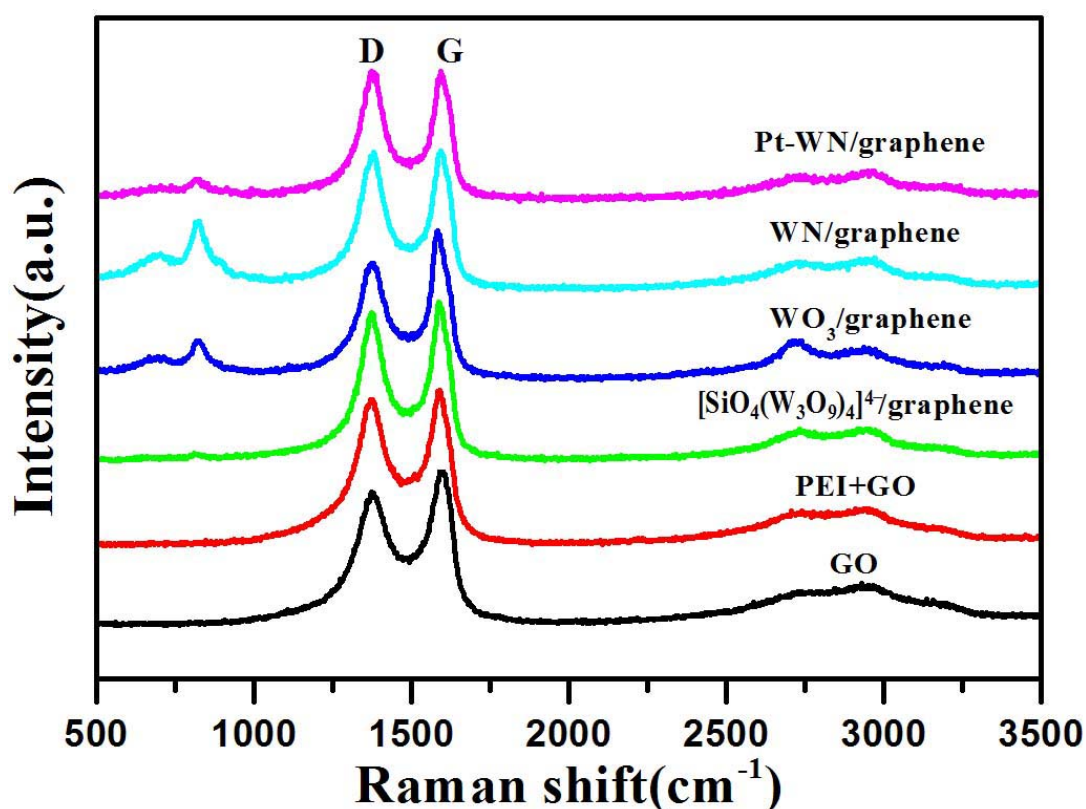*Haijing Yan, Chungui Tian*, Li Sun, Bo Wang, Lei Wang, Jie Ying, Aiping Wu, and Honggang Fu**

Figure S1. Raman spectra of GO, PEI-GO, $[Si_4(W_3O_9)_4]^{4-}$/graphene, WO_3/graphene, WN/graphene, and Pt-WN/graphene.

The Raman spectra of different samples gives two prominent peaks at 1351 cm^{-1} and 1588 cm^{-1} that correspond to D and G bands, respectively. The ratio of the intensity between the G band and D band (I_D/I_G) is usually used to measure the degree of defects present in carbon samples. We can see that the ratio of I_D/I_G have no large difference for the samples of GO, PEI-GO and SiW_{12}/graphene, indicating the slightly

reduction of GO after either PEI modification and hydrothermal treatment. The large improvement (high I_G/I_D) can be found in WO_3/graphene sample. This indicates that the calcination can remove the oxygenous groups of GO and improve the crystallinity of GO, thus resulting the formation of the GO-derived graphene. However, the ratio of I_G/I_D decrease largely for WN/graphene sample, which should be ascribed into the disordered structure induced by intensive interaction of WN and graphene, and the doping of graphene by N heteroatoms under NH_3 atmosphere. Furthermore, the peaks located at about 813 cm^{-1} (WO_3/graphene) and 820 cm^{-1} (WN/graphene) are ascribed to the stretching modes of the O-W-O [1] and W-N bond [2], respectively..

[1] Y. Baek and K. J. Yong, J. Phys. Chem. C, 2007, 111, 1213-1218.

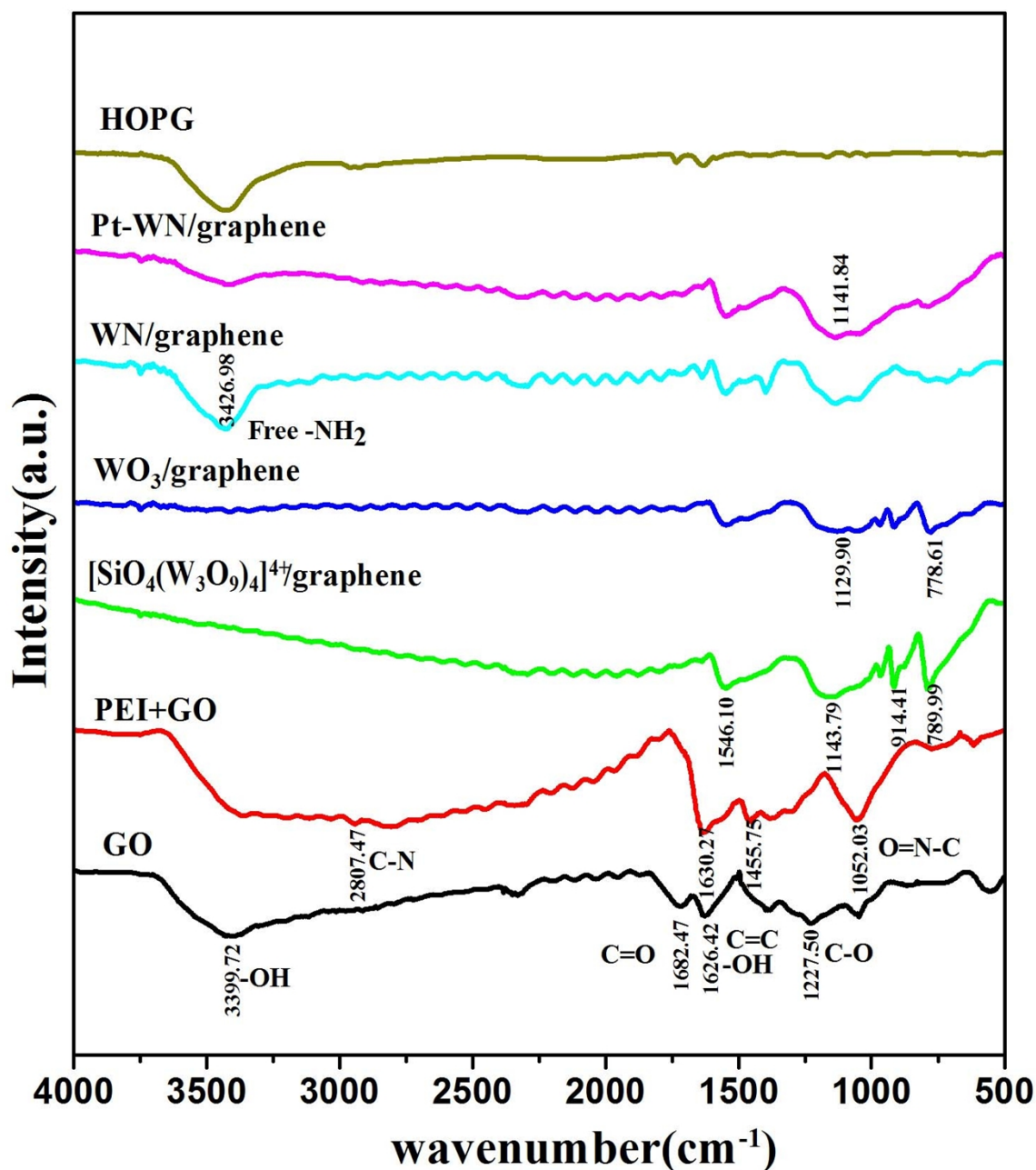[2] F. Xu, A. Fahmi, Y. Zhao, Y. D. Xia and Y. Q. Zhu, Nanoscale, 2012, 4, 7031-7037.

Figure S2. IR spectra of different samples, dark yellow: HOPG, black: GO, red: PEI-GO, green: $[Si_4(W_3O_9)_4]^{4-}$/graphene, deep blue: WO_3/graphene, light blue: WN/graphene, pink: Pt-WN/graphene.

For HOPG, the peak located at about $3400cm^{-1}$ is ascribed to the adsorption of H2O. No intensive peaks can be observed in other region. In the spectra, the peaks of

GO sample indicate the presence of O-H (3340cm^{-1}), C=O (1683 cm^{-1}) and C=C (1626 cm^{-1}). After modification with PEI, the peak ascribed to C=O-N can be found at 1500 cm^{-1}. For SiW$_{12}$-PEI-GO sample, the characteristic peaks located at 790 (W-O-W), 914 (W=O), 1144 cm^{-1} (Si-O) from SiW$_{12}$ units emerge. The peaks for W-O bond can also be observed for WO$_3$-PEI-GO sample. After the nitridation reaction, the peaks belonging to W-O-W at 790 cm^{-1} disappear. The broad peak at 1141cm^{-1} can be ascribed to the vibration of W-N bond.

The Nsp^2 is calculated by formula S1:

$$sp^2 = \frac{\left[\frac{area(\pi^*)}{area(\pi^*+\sigma^*)}\right] \text{ sample}}{\left[\frac{area(\pi^*)}{area(\pi^*+\sigma^*)}\right] \text{ 100\% sp}^2 \text{ reference, HOPG}}$$
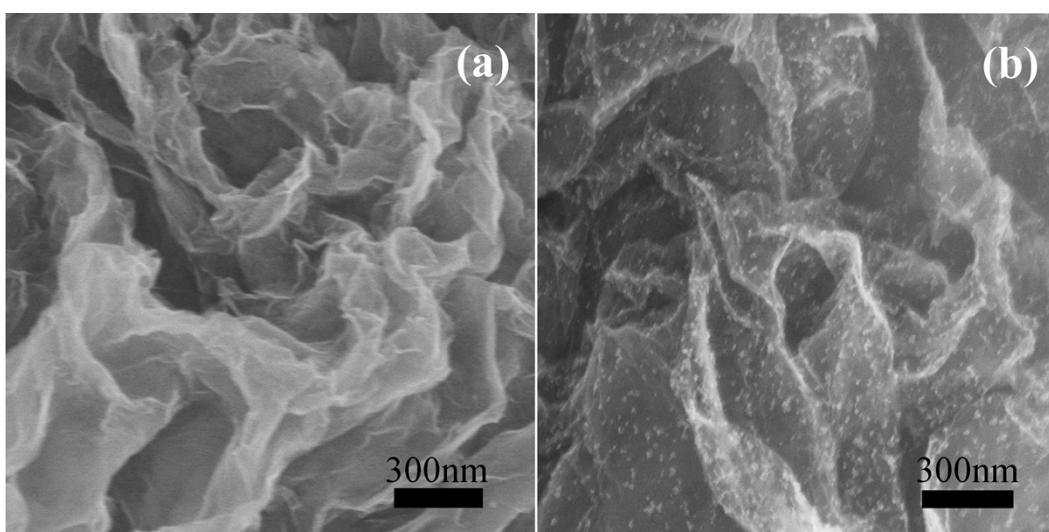
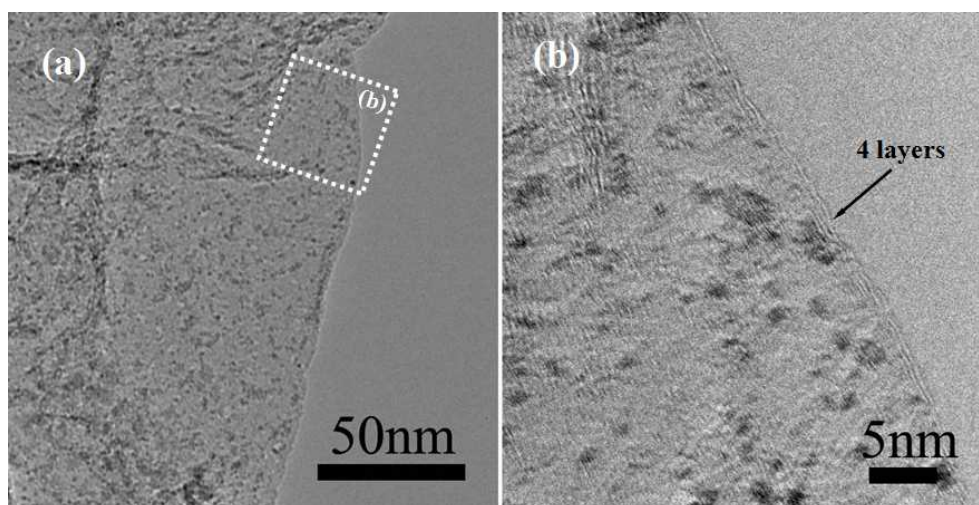**Figure S3.** SEM image (a) WN/graphene and (b) Pt-WN/graphene.

Figure S4. TEM and HRTEM images of WN/graphene in other area of TEM grids.

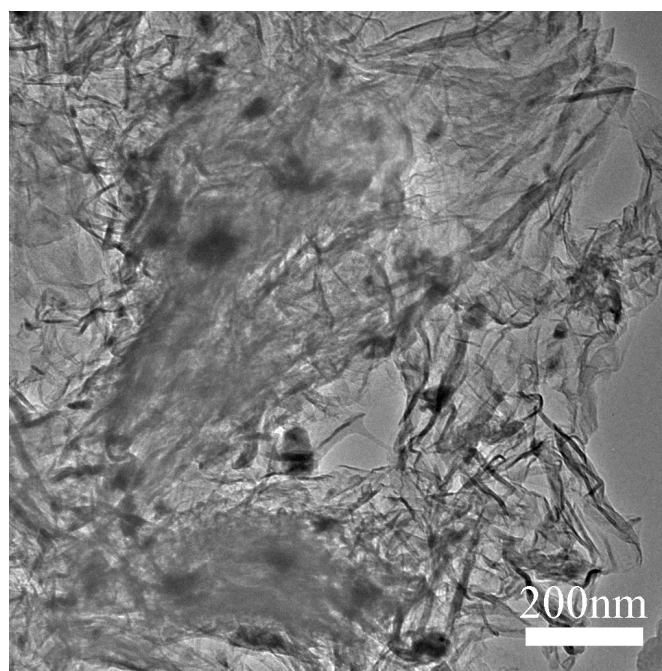We can observe the existence of graphene with 4 layers in thickness.

Figure S5. TEM image of WN/graphene prepared by using GO without PEI modification as support. It can be seen that the WN NPs are about 70 nm in size with worse uniformity than those in WN/graphene prepared by using PEI-GO as support.
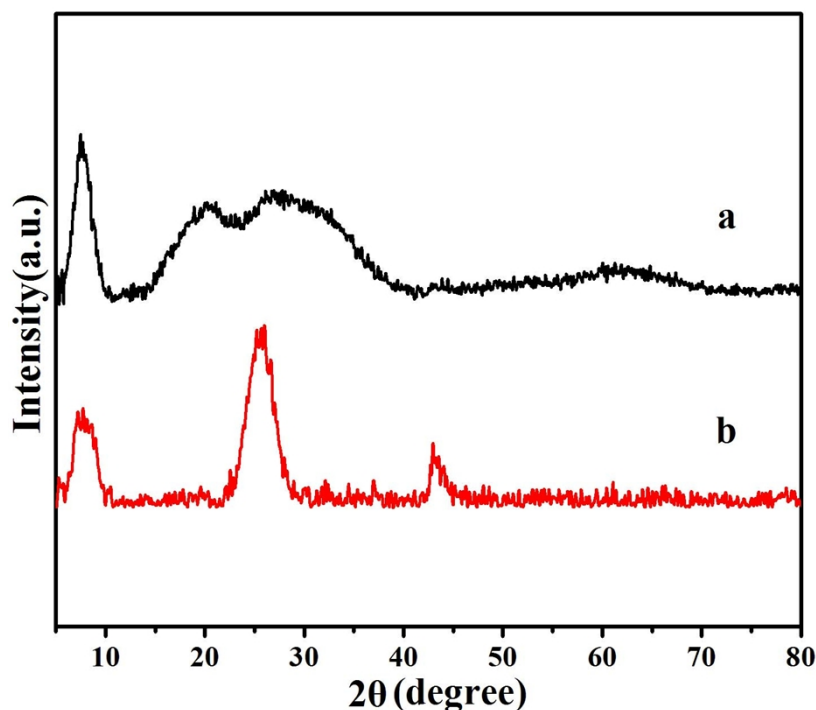
Figure S6. XRD pattern of (a) PW_{12}/graphene and (b) WO_3/graphene

Figure S6a shows the XRD pattern of PW_{12}/graphene. The peak located at $2\theta = 7.5°$ (d =11.8 Å) is from the combination of PW_{12} cluster and graphene. The size of SiW_{12} is about 8 Å. So, the distance of 11.8 Å is close to the size of PW_{12} (8 Å)+ thick of graphene sheet of 3.4 Å. No characteristic peaks corresponding to SiW_{12} are found, which should be ascribed to the the small size and homogeneous distribution of SiW_{12} species. For WO_3/graphene, the peaks located at $2\theta = 25.5°$ can be ascribed to the WO_3. The peak for graphene also emerged in this position. The peaks located at about $2\theta = 44°$ can be ascribed to the hydrated WO_3. One peak emerged at at $2\theta = 7.8°$ is ascribed to the the combination of WO_3 cluster and graphene. The shift toward to high 2θ value imply the small size of WO_3 cluster than corresponding SiW_{12}.
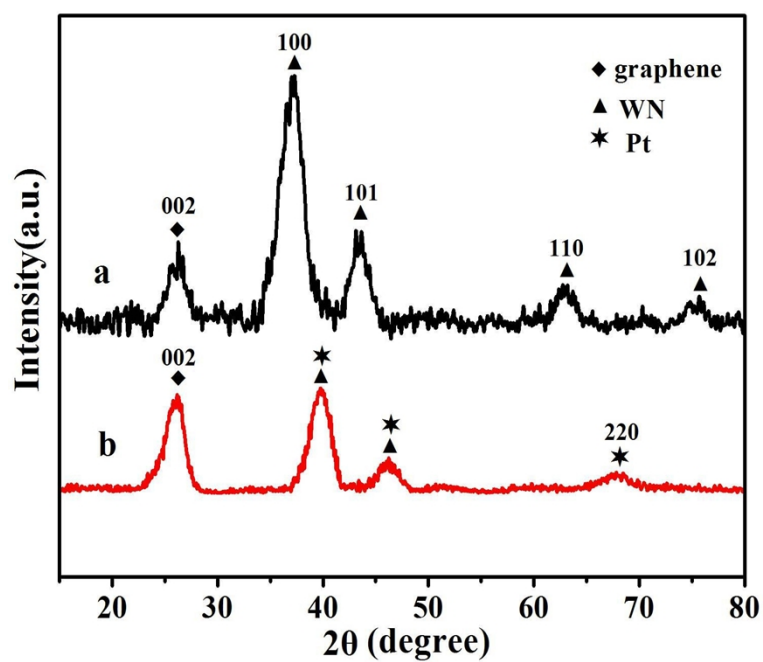
.

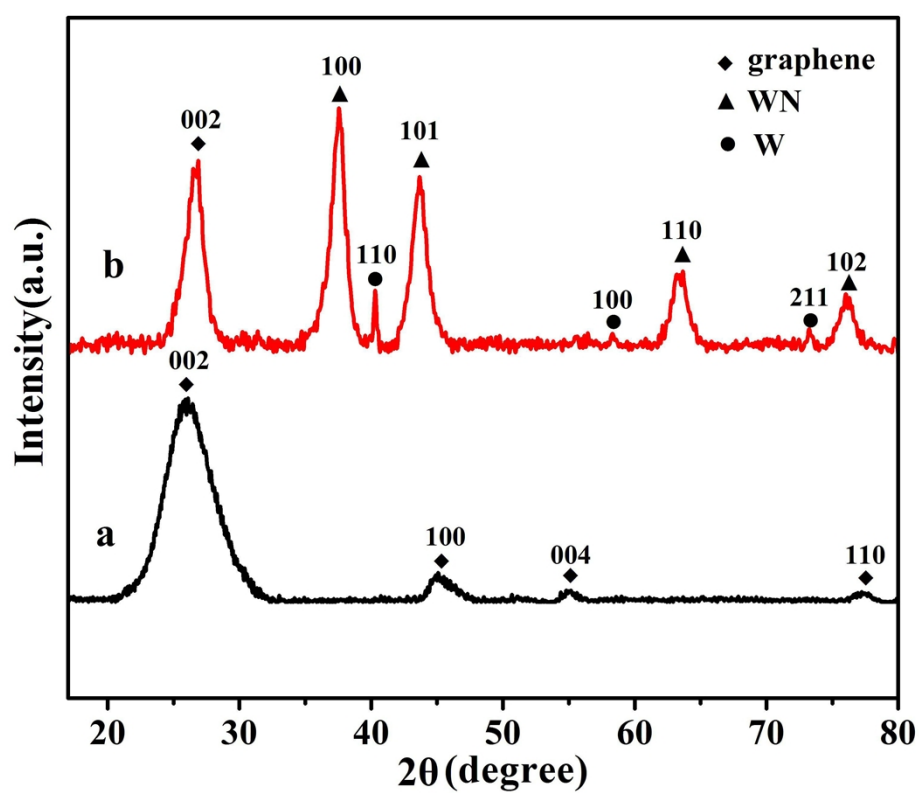**Figure S7.** XRD patterns of (a) WN/graphene (b) Pt-WN/graphene

Figure S8. XRD patterns of (a) graphene from hydrothermal treatment of GO and (b)

WN/graphene (by using GO without PEI modification as support.

In Figure S8a, the peaks at 26.48° and 54.68° are characteristic of the parallel graphene layers, whereas the 42.5° and 77.48° diffraction peaks correspond to the 2D in plane symmetry along the graphene sheets. From Figure 8b, we can see that peaks of graphene and WN. Besides, the peaks of the metal W are observed, indicating the important role of PEI for obtaining the phase-pure WN.
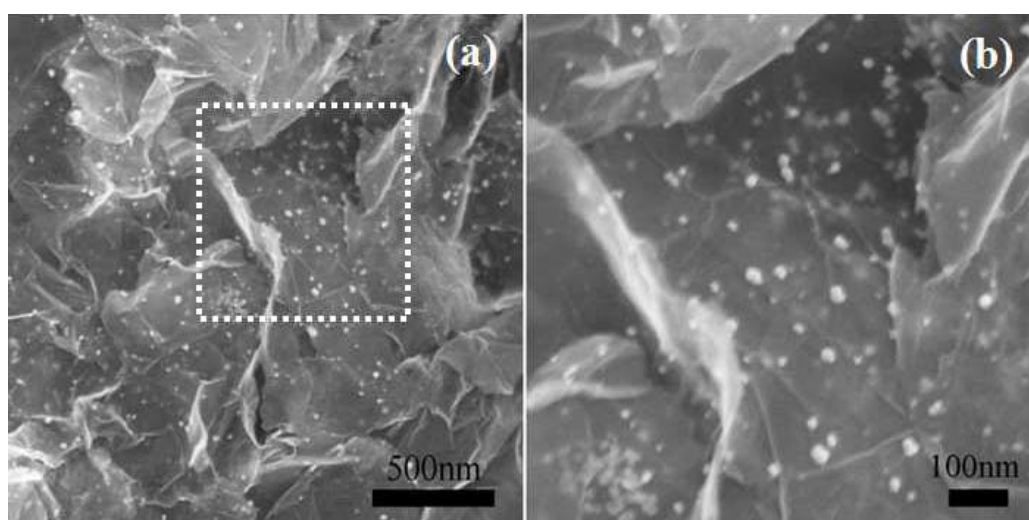

Figure S9. SEM images with different low-magnifications of Pt/graphene. The size of Pt NPs loading on the graphene is about 15 nm.

Figure S10. The C1s XPS spectra of GO.

From Figure S10, there are intensive peaks belonging to the C combined with O, which are much higher peaks than that in Pt-WN/graphene. The result indicates the removement of oxygen-containing groups in GO to form GO-derived graphene in the WN/graphene sample.
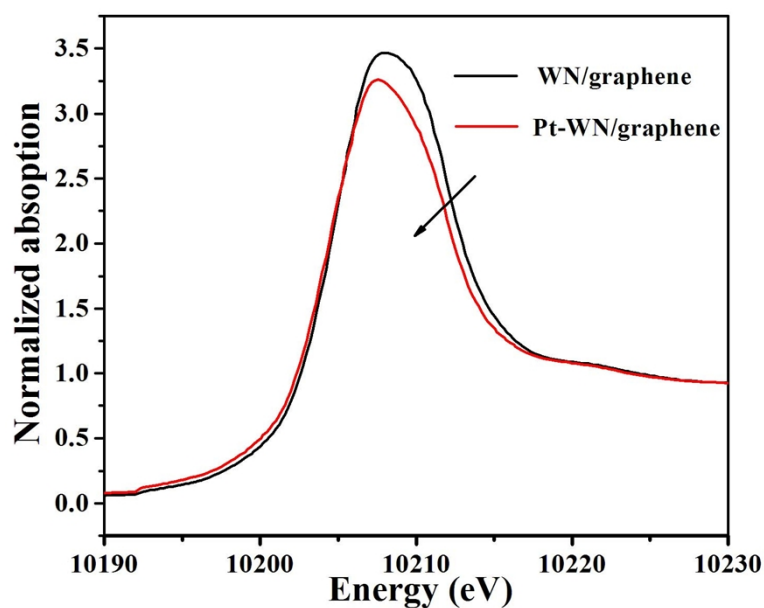

Figure S11. The W L3-edge XAFS of WN/Graphene and Pt-WN/Graphene

Figure S12. CV curves recorded in N_2-purged 1.0 M H_2SO_4 +1.0 M CH_3OH with a sweep rate of 50 mV s^{-1}. (a) WN/graphene and (b) Pt-WN/graphene by using GO without PEI modification as support.

We can clearly see that WN/graphene composites have no obvious catalytic activity. The result proofs that the WN only plays the role of a cocatalyst. At the same time, we can find that the mass activity of Pt-WN/graphene prepared by using GO without PEI modification as support is only 32.3 mA mg^{-1}_{Pt}. The result indicates the important function of PEI for producing the WN/graphene with excellent co-catalytic activity.

Table S1 S_{BET} of different catalysts

Sample	Pt-WN/graphene [*]	Pt/graphene [*]	Pt/C(JM) [1]	Pt/VC[2]	PB(JM) [3]
S_{BET} (m² g⁻¹)	263.2	50.4	170	151	28

* The S_{BET} value of Pt-WN/graphene and Pt/graphene are tested by our instrucment.

[1] The S_{BET} value is obtained from followed literature: J. Z. Zhang, K. Hongsirikarn, J. G. Goodwin Jr., *Journal of Power Sources* 2011,196, 7957-7966.

[2] The Pt/VC is Pt/Vulcan catalyst. The S_{BET} value is obtained from followed literature: F. Hasché, M. Oezaslan and P. Strasser, *Phys. Chem. Chem. Phys.*, 2010, 12, 15251-15258.

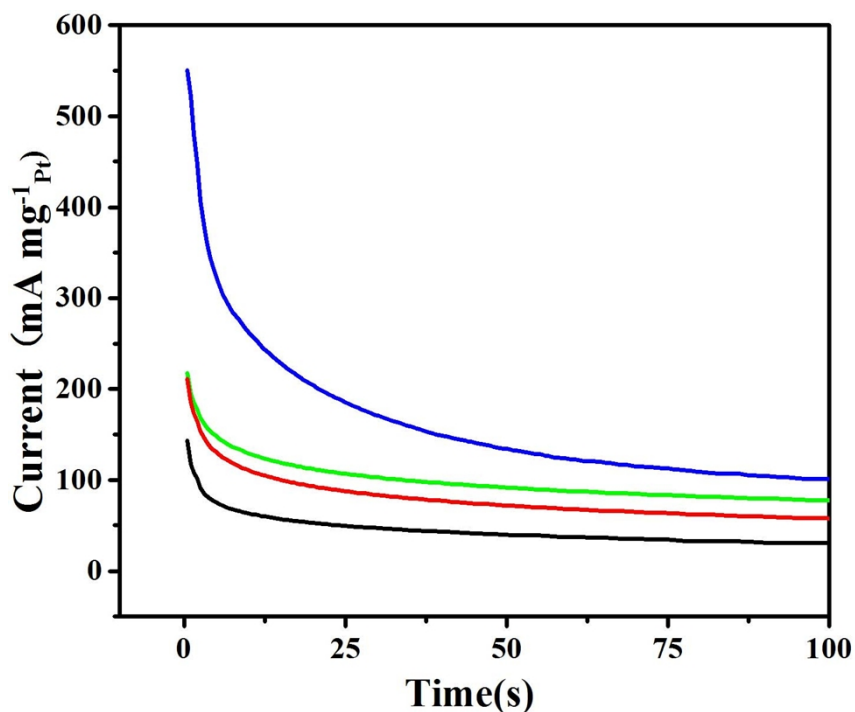[3] PB is Pt black. The S_{BET} value is obtained from the Chemical reagent Co (JM).

Figure S13. Chronoamperometric curves of different catalysts tested at 0.65V for 3600s with higher resolution at t= 0s.
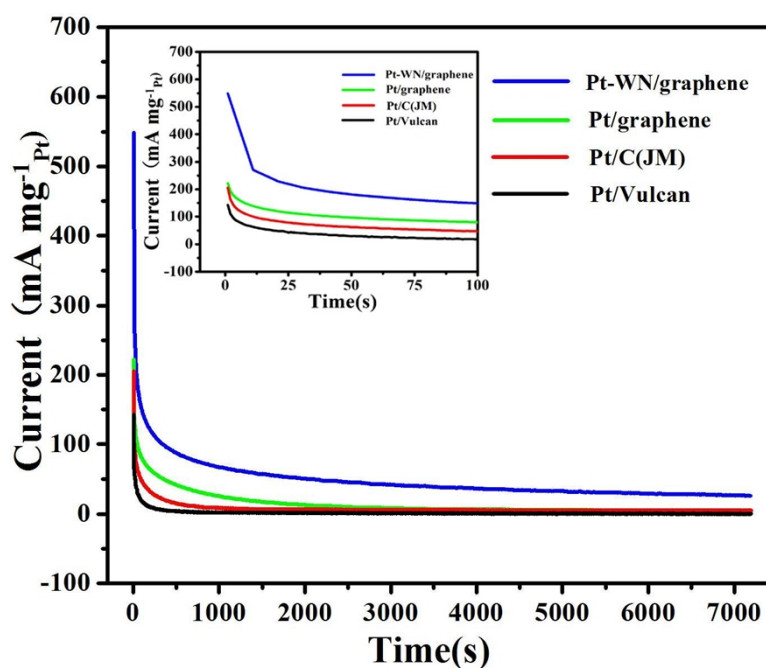
Figure S14. Chronoamperometric curves of different catalysts tested at 0.65 V. The residual currents for the Pt-WN/graphene, Pt/graphene, Pt/C(JM)and Pt/Vulcan are 26.5,19.6, 4.6 and 0.36 mA mg^{-1}$_{Pt}$ after 7200s. The inset is higher resolution curve at t= 0s.

As shown in Figure S14, after longer exposure time (7200 s), we can still see the high residual current of 26.5 mA mg^{-1}$_{Pt}$ for Pt-WN/graphene catalyst. While the values for Pt/G, Pt/C (JM) and Pt/vulcan are 9.6, 4.6 and 0.36 mA mg^{-1}$_{Pt}$ after this test. The I_7200s/I _initial are 0.048, 0.021, 0.022 and 0.0025 Pt for Pt-WN/graphene, Pt/graphene, Pt/C (JM) and Pt/vulcan, respectively, demonstrating furtherly the good stability of Pt-WN/graphene.
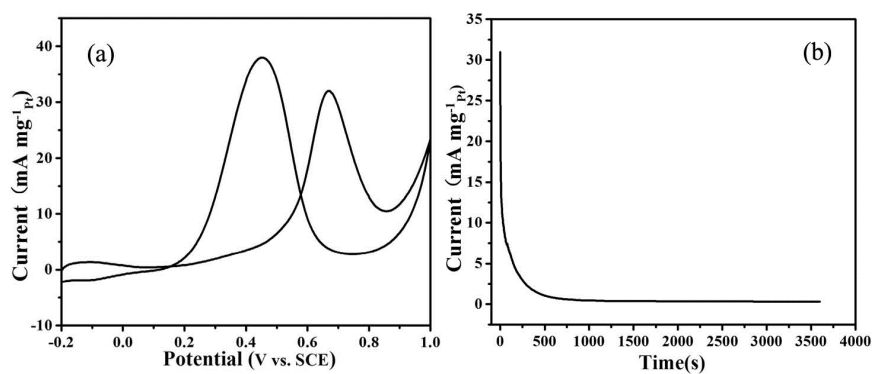
Figure S15. (a) The Cyclic voltammograms for Methanol electro-oxidation of Pt black (JM) in 1.0 M H_2SO_4 +1.0 M CH_3OH solution with a sweep rate of 50 mVs^{-1}; (b) Chronoamperometric curves of Pt black catalysts tested at 0.67V (3600s).

The mass activity of Pt black catalyst is about 32 mA mg^{-1}$_{Pt}$, much lower than that of Pt-WN/G (532 mA mg^{-1}$_{Pt}$). In addition, the residual currents for the Pt black is 0.31 mA mg^{-1}Pt after 3600s. The I_3600s/I _initial for the Pt black is about 0.00938, also much lower than that of Pt-WN/graphene (0.14).
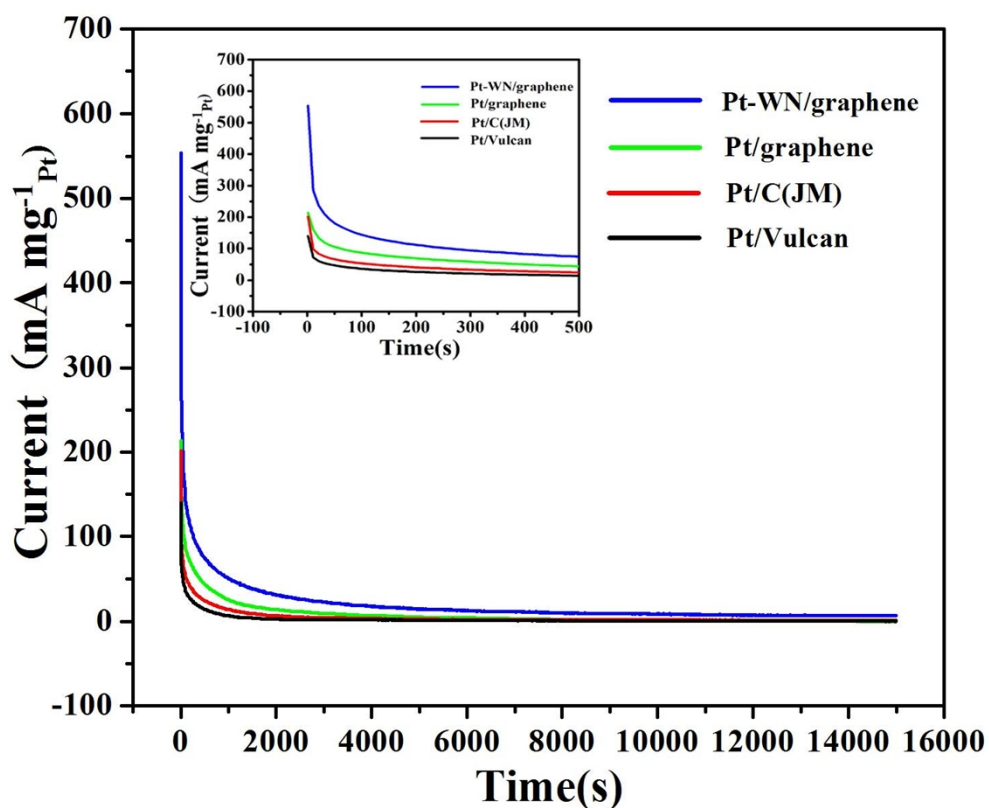
Figure S16. Chronoamperometric curves of different catalysts tested at 0.65 V.

Figure 5. Chronoamperometric curves of different catalysts tested at 0.65 V. The residual currents for Pt-WN/graphene Pt/graphene, Pt/C(JM) and Pt/Vulcan is 6.5 mA mg$^{-1}_{Pt}$, 0.03 mA mg$^{-1}_{Pt}$, 0.85 mA mg$^{-1}_{Pt}$, 0.06 mA mg$^{-1}_{Pt}$ after 15000s. The I_15000s/I _initial is about 0.012 for Pt-WN/graphene, 0.00014 for Pt/graphene, 0.004 for Pt/C(JM) and 0.00043 for Pt/Vulcan. The inset is higher resolution curve at t= 0s.
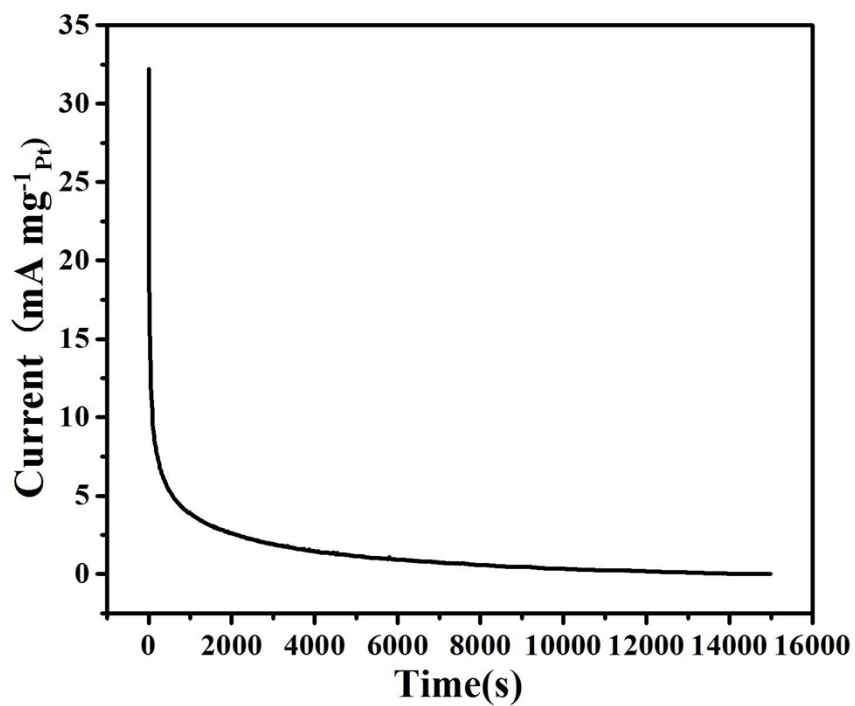
Figure S17. Chronoamperometric curves of Pt black tested at 0.65 V. The residual

currents and the I_15000s/I _initial are 0.0062 mA mg^{-1}$_{Pt}$ and 0.00019, respectiviely.
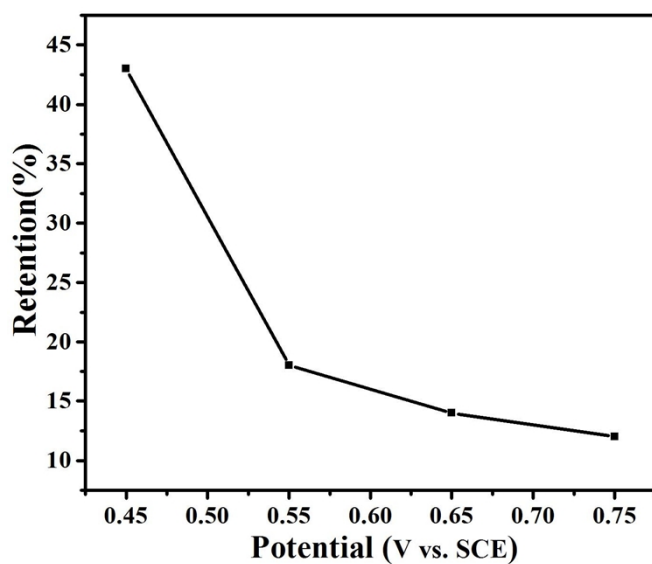

Figure S18 The potentials *vs* Retention curves of Pt-WN/graphene at different
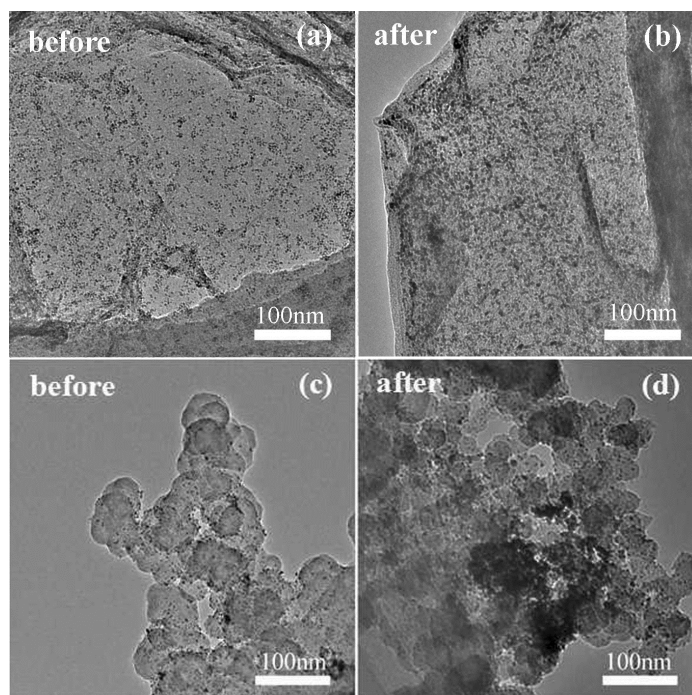
potential.

Figure S19. TEM images of (a,b) Pt-WN/graphene and (c, d) Pt/graphene catalyst before and after the electrochemical test.
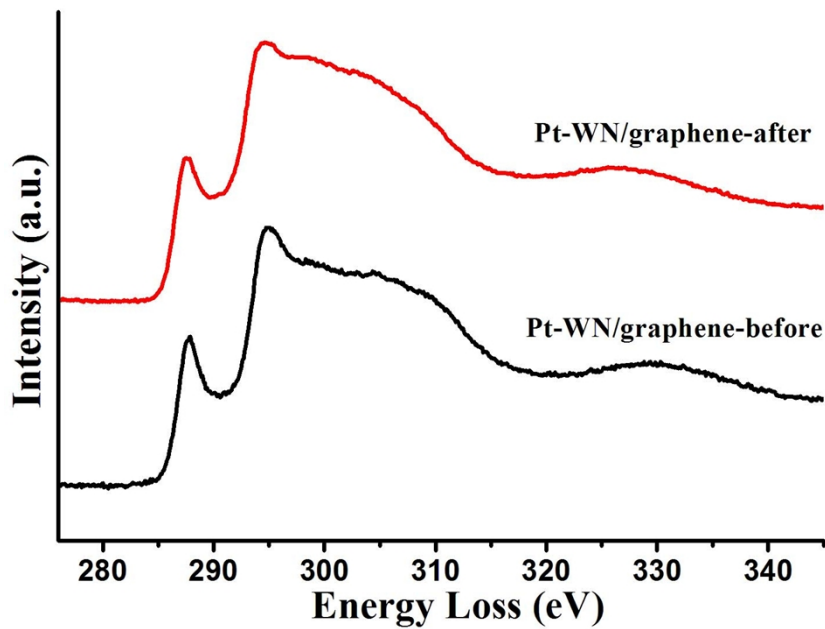

Figure S20 Carbon-K-ionization edges of Pt-WN/graphene before and after electrochemical test.

Table S2 sp^2/sp^3 quantification

	$Nsp^2(\%)$	$Nsp^3(\%)$
Pt-WN/graphene (before)	83	17
Pt-WN/graphene (after)	79	21

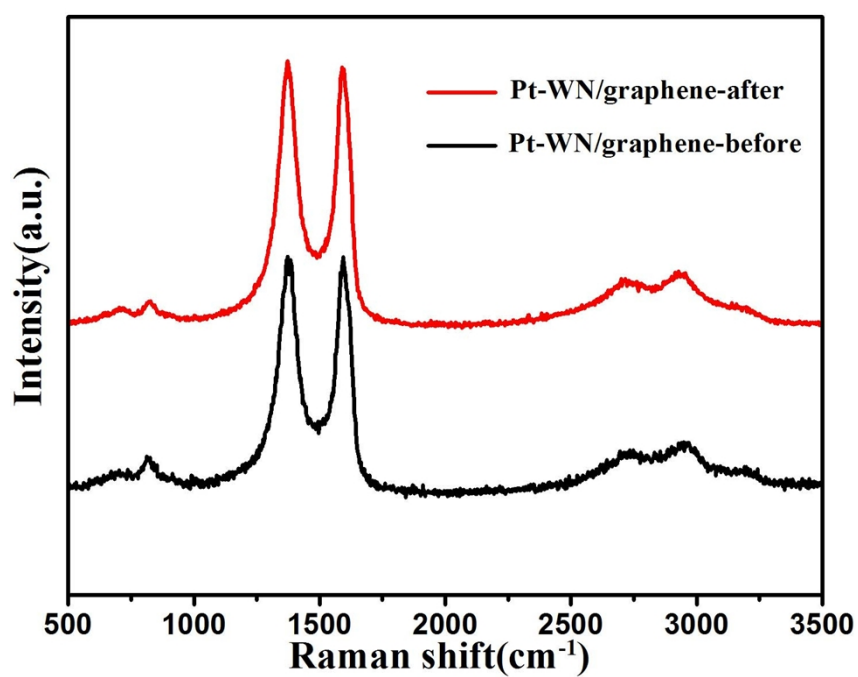**Figure S21** Raman spectra of Pt-WN/ graphene before and after electrochemical

test.